Journal of Optoelectronic and Biomedical Materials Vol. 12, No. 3, July - September 2020, p. 67 - 72

SYNTHESIS AND STRUCTURAL ANALYSIS OF InSb-CrSb, InSb-Sb, GaSb-CrSb EUTECTIC COMPOSITES

M. V. KAZIMOV*
Institute of Physics of Azerbaijan National Academy of Sciences AZ 1143, Baku, H. Javid ave., 131

İnSb-CrSb, İnSb-Sb, GaSb-CrSb eutectic composites are synthesized by the vertical Bridgman method. The existence interphase zones around metallic inclusions in GaSb-CrSb, InSb-CrSb and InSb-Sb eutectic composites have been establishedby study of the structure and elemental composition. It has been found that the peaks detected in the Raman spectra corresponded to the GaSb and InSb compounds and Sb-Sb bond.

Keywords: Eutectic composite, Structure, X-ray diffraction, Raman Scattering, SEM

(Received March 26, 2020; Accepted August 11, 2020)

1. Introduction

One of the main features of eutectic composites obtained based on InSb, GaSb and 3d - transition elements is the anisotropy in kinetic coefficients depending on the direction of metal needles. [1-4]. These composites, which combines both semiconductor and metallic properties, behave as nonhomogeneous semiconductors since metal needles are distributed parallel to the crystallization direction. The composites formed by the 3d-transition metals are considered to be diluted magnetic semiconductors. Recently, NiAs-type hexagonal structure CrSb has been widely studied as a suitable material for spintronics [5-9]. According to the results of these studies, the connection between the ferromagnetic constituents perpendicular to the crystallization axis in the CrSb junction is antiferromagnetic. Consequently consideration of the InSb-CrSb, InSb-Sb and GaSb-CrSb systems is of substantial interestl. The present paper is devoted to synthesis and structure investigated of InSb-CrSb, InSb-Sb and GaSb-CrSb eutectic composites.

2. Experimental details

2.1. Synthesis

In order to synthesize InSb-CrSb, InSb-Sb, and GaSb-CrSb eutectic composites, InSb and GaSb are first synthesized: the stoichiometric quantities of In and Sb, Ga and Sb are melted together and treated with horizontal zone alloy. The velocity along the melting zone crystallization was 12 mm/h.; the concentration of carriers in InSb and GaSb compounds was $n = 2x10^{16}$ and $p=1.8x10^{17}$ at room temperature, respectively.

Eutectics with the following mixtures: InSb and 0.6% CrSb for InSb-CrSb, InSb and 37.3% Sb for InSb-Sb, GaSb and 13.4% CrSb for GaSb-CrSb systems were filled into quartz ampoules at a pressure of 10^{-2} Pa. The ampoules were stored in an electric oven at 1200 K for 4 hours and cooled to room temperature [10-12]. At the next stage, InSb-CrSb, InSb-Sb and GaSb-CrSb composite crystallization is carried out by the vertical Bridgman method with different crystallization rates: 1.2 mm/min.; 0.6 mm/min. and 0.3 mm/min. at temperature gradient 20-30K [13].

2.2. Caracterization

The X-ray spectra of the InSb-CrSb, InSb-Sb and GaSb-CrSb composites were made by the Advance-D8 diffractometer ("Bruker"). The source of radiation was the CuKα-anode, operating at a voltage of 40 kV and a current of 40 mA. The wavelength of the radiation was λ=

* Corresponding author: m.kazimov@physics.science.az

1.5406Å, and the angle between the falling X-rays and the sample was $2\Theta = 5 \div 80$. Microstructure analysis was performed on surface of the samples parallel and perpendicular to crystallization directions by the Zeiss Sigma ™ Field Emission, SEM- Scanning Electron Microscope and the MIM-8 optical microscope.

3. Discussion

Diffraction patterns of GaSb-CrSb eutectic composite are shown in Fig. 1. Analysis of XRD spectra confirmed that this system is diphasic: the most intense peaks corresponding to the (111), (200), (220), (311), (222), (400), (331), (420), and (422) Muller index are identical to the GaSb matrix, while the weak peaks found at $2\theta = 30^{\circ}$, 44.08°, 52.12°, and 54.13° coincide with the CrSb lines having a hexogonal structure with lattice parameters of a = 4.121, c = 5.467, c/a = 1.327, and the P63/mmc space group.

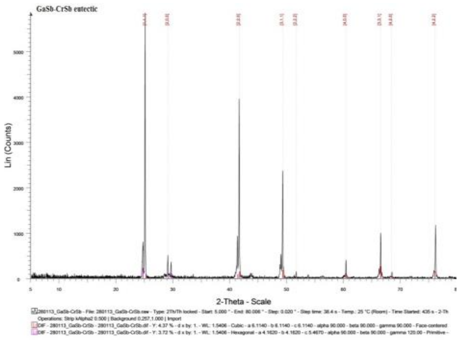

Fig. 1. X-ray spectrum of GaSb-CrSb eutectic composite.

Fig. 2 shows the diffraction patterns of the InSb-CrSb eutectic composite. The most intense peaks corresponding to the (111), (220), (311), (400), (311), (422) və (511) Muller index are identical to the InSb matrix, while the weak peaks found at $2\theta = 30^{\circ}$, 44.08°, 52.12°, and 54.13° coincide with the CrSb line.

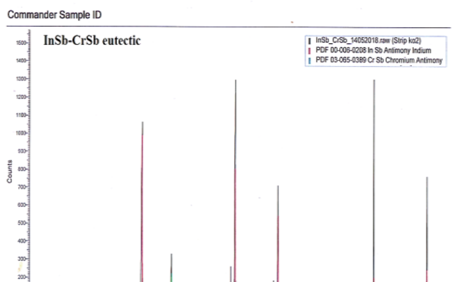

Fig. 2. X-ray spectrum of InSb-CrSb eutectic composite.

Fig. 3 shows the diffraction patterns of the InSb-Sb eutectic composite. The most intense peaks corresponding to the (111), (220), (311), (400), (311), (422) və (511) Muller index are identical to the InSb matrix, while the weak peaks found at $2\theta = 30^{\circ}$, 44.08°, 52.12°, and 54.13° coincide with the CrSb line.

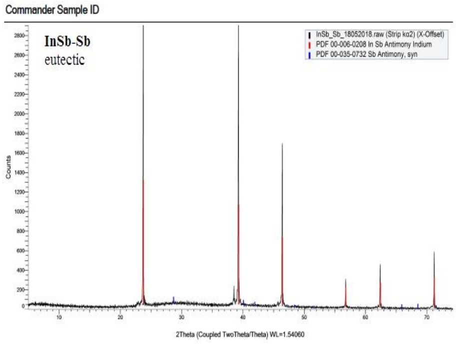

Fig. 3. X-ray spectrum of InSb-Sb eutectic composite.

Shown in Fig. 4 the structure of the films is it can be seen structural formations of a round shape are evenly distributed on the surface of the film.

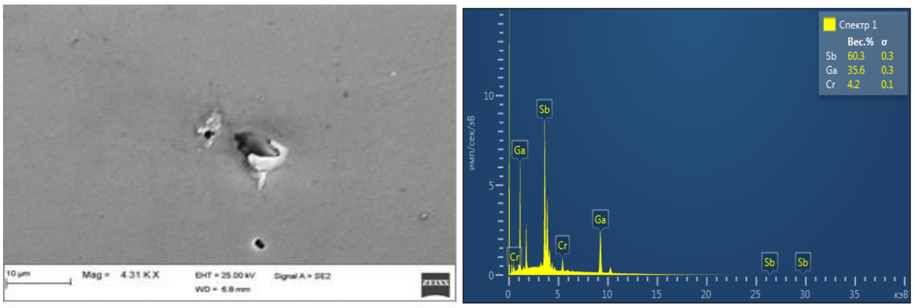

Fig. 4. X-ray spectra of GaSb–CrSb thin film obtained with SEM–EDX.

The length of the metal rods (1-1.6 µm in diameter) is 10-100µm in InSb-CrSb composite, 30-50 µm in GaSb-CrSb, 40-100µm in InSb-CrSb. As it is seen from Fig. 4, the metal rods are evenly distributed in the matrix in the direction of crystallization.

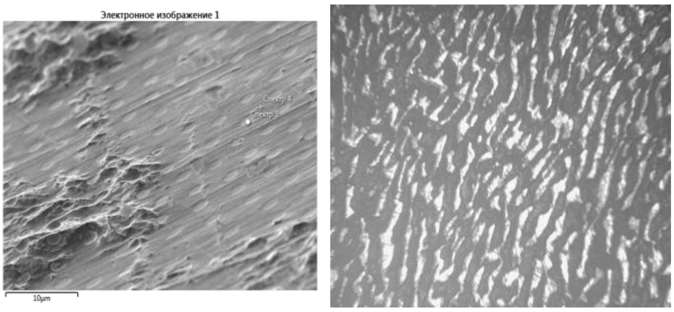

(a)

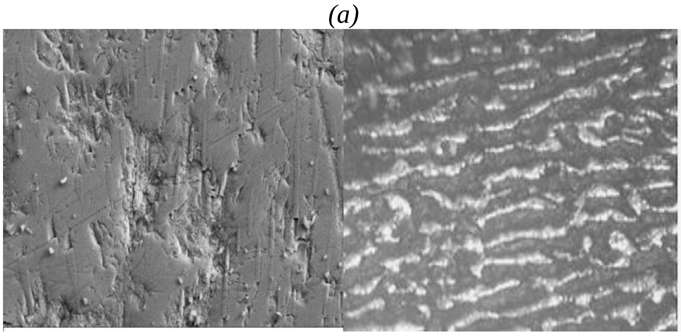

(b)

Fig. 5. SEM micrographs of GaSb-CrSb and InSb-CrSb eutectic alloys showing cross sections of the samples along the longitudinal and lateral directions of the CrSb phase.

Fig. 4 shows an element map of the GaSb-CrSb eutectic alloy. In the specific map, the colours red, blue and green indicate Sb (L), Cr (K) and Ga (K), respectively and black colour indicates the absence of this element.

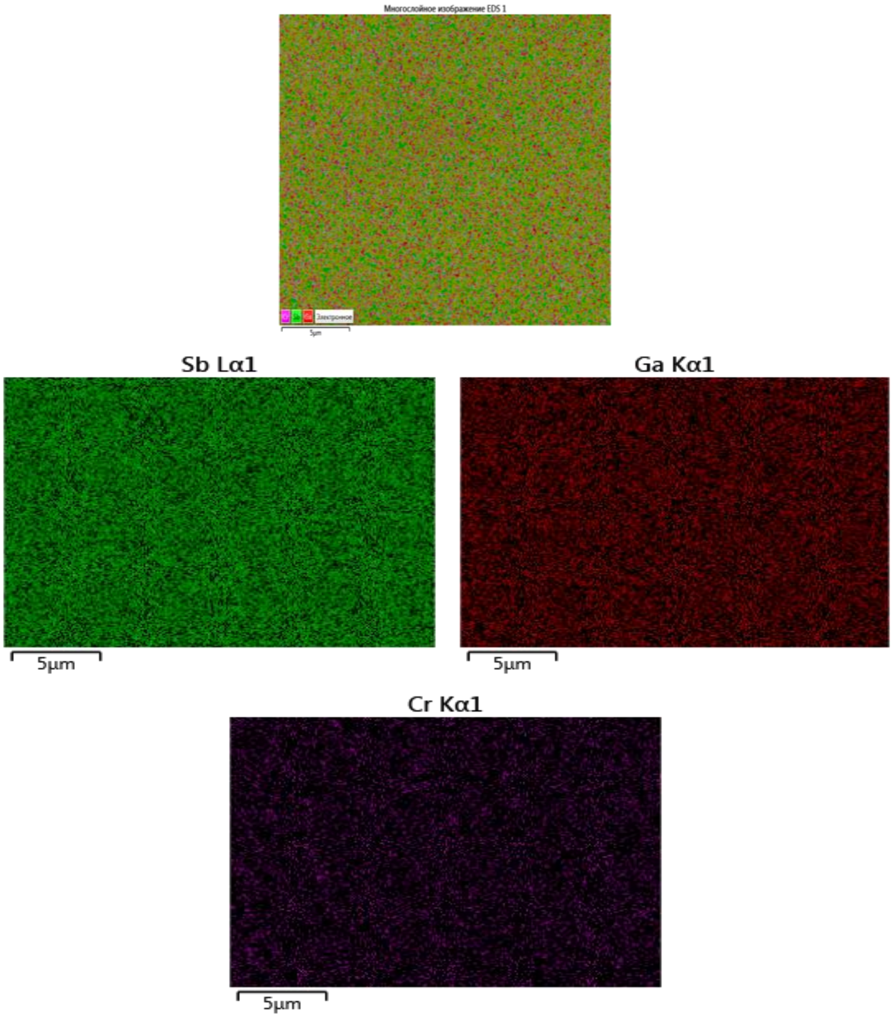

Fig. 6. Element map of the GaSb–CrSb composite.

Some parameters of semiconductor-metal type InSb-CrSb, InSb-Sb, and GaSb-CrSb eutectic composites are shown in the Table [6,7,11].

Eutectic composites	Metal phase weight %	Needles density, mm^{-2}	Needles diameter, μm	Needles length, μm	Crystallization speed, mm/min	Concentration, cm^{-3}
GaSb-CrSb	13,4	$5,2x10^4$	1,4	30-50	0,3-0,6	$p=8x10^{17}$
InSb-CrSb	0,6	$0,6x10^4$	1	100-200	1,2	$p=2x10^{17}$
InSb-Sb	37,6	$2,5x10^4$	1,6	40-100	1,4	$p= 10^{17}$

Raman analysis is an important tool to study atomic interactions in semiconductors and the dynamics of the crystal lattice [14-16]. Raman analysis were investigated to confirm the existence of two-phase and inter-phase zones in the GaSb-CrSb, InSb-CrSb, InSb-Sb eutectic composites at room temperature. Fig.7 and Fig.8 shows the Raman lines at about 111cm-1, 148cm-1, 230cm-1, 240cm-1 are the mode LO GaSb-CrSb eutectic composite, and 114cm-1, 154cm-1, 240cm-1 for CrSb compound.

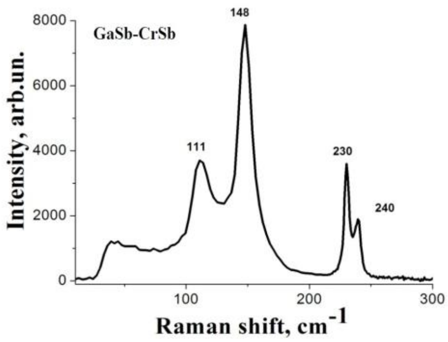

Fig. 7. Raman spectra of GaSb-CrSb eutectic composite.

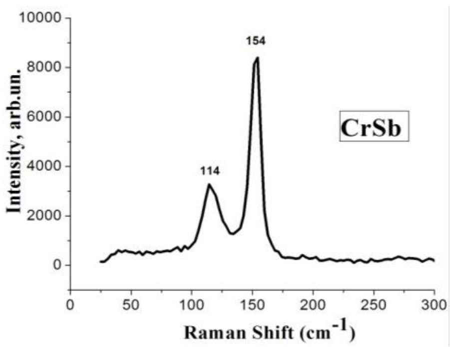

Fig. 8. Raman spectra of CrSb compound.

Fig. 9 (a) and (b) are shows the Raman lines about InSb-CrSb composite are 101cm-1, 145cm-1, 174cm-1 and (b), respectively, at 101cm-1, 150cm-1 and 240cm-1.

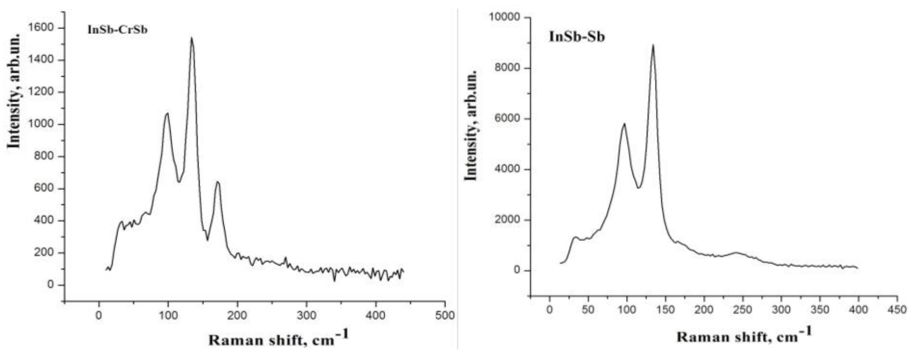

(a) (b)

Fig. 9. Raman spectra of InSb-CrSb (a) and InSb-Sb (b) eutectic composites.

4. Conclusions

Thus, X-phase analysis of InSb-CrSb, GaSb-CrSb and InSb-Sb alloys is a composite composite comprising matrix (InSb and GaSb) and porous metal coatings (CrSb and Sb) based on studies in optical and electron microscopes. The Raman spectra obtained in the InSb-CrSb and GaSb-CrSb compositions only characterize the Sb-Sb bond [15,17].

References

[1] M. V. Kazimov, D. H. Arasly, R. N. Rahimov, A. A. Khalilova, I. K. Mammadov, Journal of Non-Oxide Glasses **5**(1), 7 (2020).

[2] J. A. Graves Undercooling and Solidification Behavior in the InSb-Sb System, NASA CR-175013, September 1985, p.216.

[3] M. V. Kazimov, D. H. Arasly, I. Kh. Mammadov, R. N.Rahimov, A. A. Khalilova, Azerbaijan Journal of Physics **24**(3), 29 (2018).

[4] R. N. Rahimov, M. V. Kazimov, D. H. Arasly, A. A. Khalilova, I. Kh. Mammadov, Journal Ovonic Research **13**(3), 113 (2017).

[5] Yong Liu, S. K. Bose, J. Kudrnovsky, World Journal of Engineering **9**, 125 (2012).

[6] S. Polesya, G. Kuhn, S. Mankovsky, H. Ebert, M. Regus, W. Bensch, J. Phys. Condens. Matter. **24**(3), 2012.

[7] M. Shirai, J. Appl. Phys. **93**(10), 2003.

[8] Yong Liu, S. K. Bose, J. KudrnovskyWorld Journal of Engineering **9**, 125 (2012).

[9] CrSb, physical properties, Springer & Material Phases Data System (MPDS), Switzerland & National Institute for Materials Science (NIMS), (2013).

[10] A. Müller, M. Wilhem, J. Phys. Chem. Solids **26**, 2029 (1965).

[11] N. Wang, Y. Cai, R. Q. Zhang, Materials Science Engineering: Review Reports **60**(1-6), 1 (2008) .

[12] Y. Umehara, S. Koda, J. Japan Inst. Metals **50**, 666 (1986).

[13] M. I. Aliyev, A. A. Khalilova, D. H. Arasly, R. N. Rahimov, M. Tanoglu, L. Ozyuzer, J. Phys. D: Appl. Phys. **36**, 2627 (2003).

[14] F. M. Liu et al., Submitted to Journal of Physics: Condensed Matter, 2001.

[15] C. E. M.Campos, P. S. Pizani, Journal of Applied Physics **89**, 3631 (2001).

[16] S. Winnerl, S. Sinning, T. Dekorsy, M. Helm, Applied Physics Letters **85**, 30923094 (2004).

[17] M. R. Joya, P. S. Pizania, R. G. Jasinevicius, J. Appl. Phys. **100**, 053518 (2006).